NANO LETTERS

2005
Vol. 5, No. 4
803−807

Detection Limits for Nanoscale Biosensors

Paul E. Sheehan* and Lloyd J. Whitman

Chemistry Division, Naval Research Laboratory, Washington, D.C. 20375

Received February 15, 2005

ABSTRACT

We examine through analytical calculations and finite element simulations how the detection efficiency of disk and wire-like biosensors in unmixed fluids varies with size from the micrometer to nanometer scales. Specifically, we determine the total flux of DNA-like analyte molecules on a sensor as a function of time and flow rate for a sensor incorporated into a microfluidic system. In all cases, sensor size and shape profoundly affect the total analyte flux. The calculations reveal that reported femtomolar detection limits for biomolecular assays are very likely an analyte transport limitation, not a signal transduction limitation. We conclude that without directed transport of biomolecules, individual nanoscale sensors will be limited to picomolar-order sensitivity for practical time scales.

Tremendous progress is being made in the development of microanalytical systems for biosensing, driven by parallel advances in biotechnology, microtechnology, and microfluidics.[1,2] The advantages of small, highly integrated systems include more rapid and multiplexed analysis and reagent sample volumes reduced to the microliter range. When combined with innovative signal transduction technology, microsystems have recently achieved specific biomolecular detection at roughly femtomolar (fM) concentrations, corresponding to just a few thousand (or even a few hundred) analyte molecules in the sample volume.[3−5] Concurrently, many research groups have been developing micrometer or nanometer scale sensing elements based on novel transduction mechanisms.[5−11]

Many researchers of nanometer-scale phenomena focus on the fact that miniaturizing a sensor often increases its signal-to-noise ratio (S:N), an inherent advantage for signal transduction, but the effect of nanoscale miniaturization on the overall sensitivity, which includes mass transport effects, has not been widely considered. For example, whether nanometer-scale sensors are intrinsically more sensitive overall than micrometer-scale sensors has not been fully examined. In this letter, we use experimentally verified[12−14] analytical solutions to examine the maximum sensitivity with which micro-to-nanoscale sensors of various geometries can detect biomolecules from solution. Our principal goal is to explicitly examine mass transport effects on biosensing at the nanoscale; however, the calculations also lead us to conclude that reported femtomolar detection limits for bioassays are likely an analyte transport limitation, not a signal transduction limitation. The implication is that, without methods to actively direct biomolecules to a sensor surface, individual nanoscale sensors will be subject to picomolar-order detection limits for practical time scales.[15]

In the past decade, several papers have analyzed the effect of flow,[16−18] size,[13] or adsorption isotherms[19] on biomolecular adsorption; however, none have explicitly examined the effect at nanometer length scales. This effect is most easily examined using a simple geometry—a single hemisphere that protrudes from a plane (Figure 1 inset) and that irreversibly adsorbs analyte. Irreversible adsorption is a useful assumption in that it establishes an *upper bound* to the number of molecules that can accumulate on a sensor and, in practice, is a reasonable approximation for a strongly binding molecule such as DNA. Using this model, one may determine the maximum number of molecules attached to the hemisphere as a function of time, i.e., the accumulation N, defined[20] as

$$N(t) = \int_0^t J(\tau)\,\mathrm{d}\tau = \int_0^t \int_A \int j\,\mathrm{d}\sigma\,\mathrm{d}\tau \qquad (1)$$

where J is the total flux (molecules s^{-1}), j is the flux at the sensor (molecules s^{-1} m^{-2}), σ is a unit area, A is the sensor area, and t is time. For sensors that require a threshold number of molecules for detection, the accumulation is more important than the flux because it determines how quickly that threshold is reached.

For a hemispherical sensor, the accumulation is uniform across the surface and is given by

$$N(a,t) = 2\pi N_A c_0 D\left(at + 2a^2\sqrt{\frac{t}{\pi D}}\right) \qquad (2)$$

where N_A is Avogadro's number, c_0 is the initial solution

* Corresponding author. E-mail: paul.sheehan@nrl.navy.mil.

10.1021/nl050298x
Published on Web 03/08/2005

Report Documentation Page

Form Approved
OMB No. 0704-0188

1. REPORT DATE	2. REPORT TYPE	3. DATES COVERED
FEB 2005		**00-00-2005 to 00-00-2005**

4. TITLE AND SUBTITLE	5a. CONTRACT NUMBER
Detection Limits for Nanoscale Biosensors	5b. GRANT NUMBER
	5c. PROGRAM ELEMENT NUMBER
6. AUTHOR(S)	5d. PROJECT NUMBER
	5e. TASK NUMBER
	5f. WORK UNIT NUMBER
7. PERFORMING ORGANIZATION NAME(S) AND ADDRESS(ES) **Naval Research Laboratory,Chemistry Division,4555 Overlook Avenue SW,Washington,DC,20375**	8. PERFORMING ORGANIZATION REPORT NUMBER
9. SPONSORING/MONITORING AGENCY NAME(S) AND ADDRESS(ES)	10. SPONSOR/MONITOR'S ACRONYM(S)
	11. SPONSOR/MONITOR'S REPORT NUMBER(S)

12. DISTRIBUTION/AVAILABILITY STATEMENT
Approved for public release; distribution unlimited

13. SUPPLEMENTARY NOTES

14. ABSTRACT

We examine through analytical calculations and finite element simulations how the detection efficiency of disk and wire-like biosensors in unmixed fluids varies with size from the micrometer to nanometer scales. Specifically, we determine the total flux of DNA-like analyte molecules on a sensor as a function of time and flow rate for a sensor incorporated into a microfluidic system. In all cases, sensor size and shape profoundly affect the total analyte flux. The calculations reveal that reported femtomolar detection limits for biomolecular assays are very likely an analyte transport limitation, not a signal transduction limitation. We conclude that without directed transport of biomolecules, individual nanoscale sensors will be limited to picomolar-order sensitivity for practical time scales.

15. SUBJECT TERMS

16. SECURITY CLASSIFICATION OF:			17. LIMITATION OF ABSTRACT	18. NUMBER OF PAGES	19a. NAME OF RESPONSIBLE PERSON
a. REPORT	b. ABSTRACT	c. THIS PAGE			
unclassified	**unclassified**	**unclassified**	**Same as Report (SAR)**	**5**	

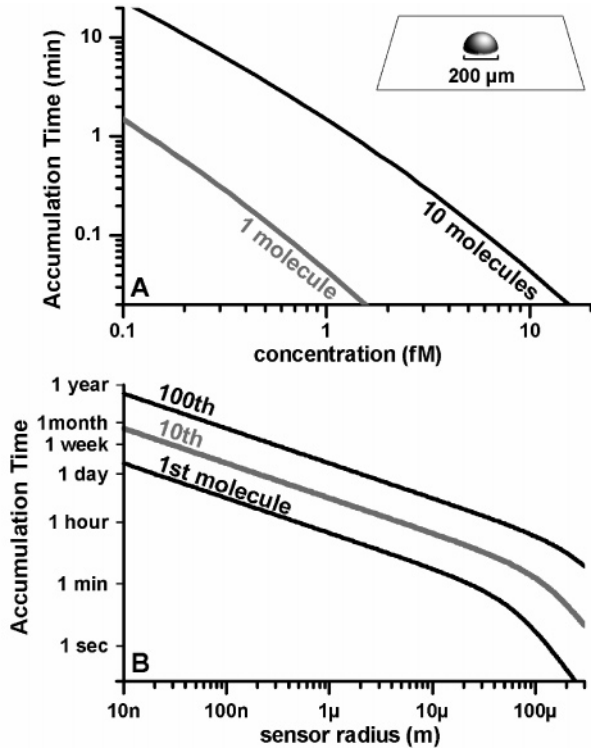

Figure 1. (A) Time required to accumulate one or 10 analyte molecules via static diffusion onto a 200 μm-diameter hemisphere for a diffusion constant of 150 $\mu m^2\ s^{-1}$, characteristic of single-stranded DNA approximately 20 bases long. After one minute, a few molecules can be expected on the sensor for a sample concentration of 1 fM. The inset shows the sensor geometry. (B) Time required for this sensor to accumulate 1, 10, and 100 molecules when submerged in a semi-infinite 1 fM solution. For radii smaller than 10 μm the required time varies linearly with the radius.

concentration, and a is the radius of the hemisphere. For this and the other examples to be discussed, we will use a diffusion constant, D, of 150 $\mu m^2\ s^{-1}$, corresponding to that for single-stranded DNA about 20 nucleotides long.[21] Equation 2 may be used to answer the following practical question: if every analyte molecule that contacts the sensor surface (or spot of capture probes) could be detected, what is the minimum detectable concentration for a given accumulation time? Figure 1A shows the results for a 200 μm diameter hemisphere (typical of a DNA microarray), revealing in this case that the minimum concentration to detect a few molecules in ~1 min is ~1 fM, which (we believe not coincidentally) is roughly the state of the art for DNA detection (~20 fM).[3,4] Figure 1B uses the same equation to illustrate the time required to achieve 1 fM sensitivity for smaller sensors. For radii below ~10 μm, the first term within the parentheses in eq 2 dominates, making the accumulation proportional to the radius. The second term within the parentheses produces a transient enhancement for larger sensors at shorter times.

A more realistic geometry for a microelectronic sensor [22] or a DNA microarray spot[23] is a disk-shaped sensing region within a flat surface, a geometry that significantly complicates the mathematics. Fortunately, analytical solutions to many diffusion problems are often analogous to those known

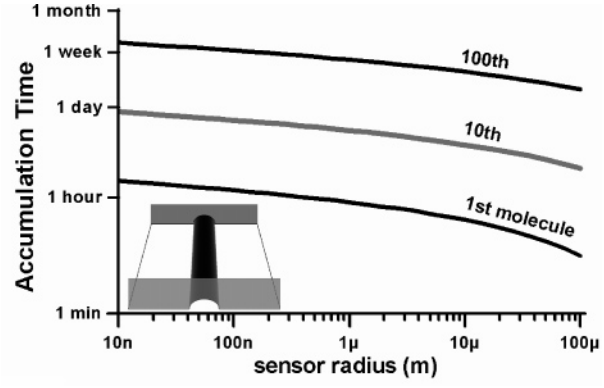

Figure 2. Time required for a 10 μm long hemicylindrical sensor to accumulate 1, 10, and 100 molecules. The sensor lies at the bottom of a channel whose width is equal to the sensor's length and which is filled with a 1 fM analyte solution. For radii smaller than ~10 μm, the required time varies linearly with the radius. The inset shows the sensor geometry.

from analysis of heat transfer or electrostatics. In this case, the solution for the steady state flux to a circular area is similar to that in the "Weber's disk" problem in electrostatics,[24]

$$j(r) = \frac{2DN_A c_0}{\pi\sqrt{a^2 - r^2}} \tag{3}$$

where r is the distance from the center of the disk. Unlike the hemispherical case, the flux increases with the radius and is significantly enhanced at the edges ($r \approx a$).[25] Integrating this flux with eq 1 yields the steady-state accumulation of

$$N(t) = 4DN_A c_0 at \tag{4}$$

which is linear in both radius and time and quite similar to the steady-state solution for smaller hemispheres. One principal difference is that for a disk and a hemisphere of the same area, the disk accumulates ~11% less in steady state, a phenomenon known in the analogous heat transfer problem as constrictive resistance.[26] That these two very similar objects behave differently should be a reminder that the sensor *shape* is also an important design consideration.

Given recent advances in the use of nanowires[6] and nanotubes[7] as biosensors, we chose to consider a final geometry—a cylindrical sensor oriented perpendicular to a channel (Figure 2). Because the nanowire/nanotube typically resides on a surface (which occludes flux from below), it may be approximated as a hemicylinder of length, l, and radius, a. The accumulation is given by

$$N(t) = \frac{4lN_A c_0}{\pi}\int_0^\infty \frac{1 - e^{-Du^2 t}}{J_0(au)^2 + Y_0(au)^2}\frac{du}{u^3} \tag{5}$$

where J_0 and Y_0 are Bessel functions. Figure 2 plots the time required to accumulate 1, 10, and 100 molecules from a 1

fM solution, revealing a much weaker dependence on radius for this geometry than for a hemisphere or disk. This difference is a consequence of the fixed length of the hemicylinder: only two dimensions are being varied and not three. This indicates that the sensor length, l, is the critical dimension for a hemicylinder since accumulation increases linearly (eq 5) with increasing length but only weakly with radius ($N \propto a^{<0.25}$ for practical time scales). Thus, sensitivity will be increased by using longer structures if the transduction signal-to-noise does not decrease more than linearly with length. Moreover, there is little penalty for reducing the wire radius if the S:N can be improved thereby.

The fundamental obstacle facing the smallest sensors is seen in these first two figures. For example, in Figure 1B, if we assume that ~10 molecules are required for reliable detection, at 1 fM the average time required to accumulate a sufficient number of molecules on a submicron hemispherical sensor exceeds any reasonable assay time (i.e., days). Even when long detection times are acceptable, the stability of the measurement can become an issue because of other effects, such as nonspecific adsorption, desorption of previously captured molecules, sample degradation, and the stochastic nature of measuring only a few molecules. The situation worsens for molecules with smaller diffusion constants. For example, proteins with molecular weights ~100 kDa (e.g., antibodies) diffuse about an order of magnitude slower, so the accumulation would be ~10 times less; the accumulations shown would require ~10 fM, or ~1 pg/mL.

Although it is clear from the recent literature that mass transport limitations deserve wider consideration, many scientists have encountered these limitations and have therefore developed methods for enhancing the total flux to the sensor. For instance, analyte molecules can be actively directed toward the sensor via electrostatic fields, a method which has been demonstrated for nucleic acids and proteins.[27] Similarly, target molecules can be attached to magnetic particles that are then directed toward the sensor via magnetic field gradients.[9] Finally, the sensitivity limitations inherent to smaller sensors could be overcome through large-scale integration of many sensors into a closely packed array (assuming it can be kept small enough to work within a microfluidics system).

Flowing sample past the sensor is one method of increasing the flux; however, the enhancement becomes marginal for nanosensors. Although fluid flow significantly complicates the mathematics, approximate analytical solutions exist[13] (see Supporting Information) for some simple configurations such as a disk (Figure 3) or a nanowire-like hemicylindrical sensor aligned perpendicular to the flow channel (Figure 4). These two figures show that increasing the flow rate increases the flux to both wires and disks with the effect being more pronounced for disks. The relative enhancement, however, decreases rapidly with sensing area. For example, whereas the total flux to a 100 μm radius sensor (Figure 3) can easily be increased by a factor of thirty, increasing the total flux to a 1 μm sensor is very difficult. Even at 1000 μL/min (a difficult flow rate to achieve in practice) total flux is

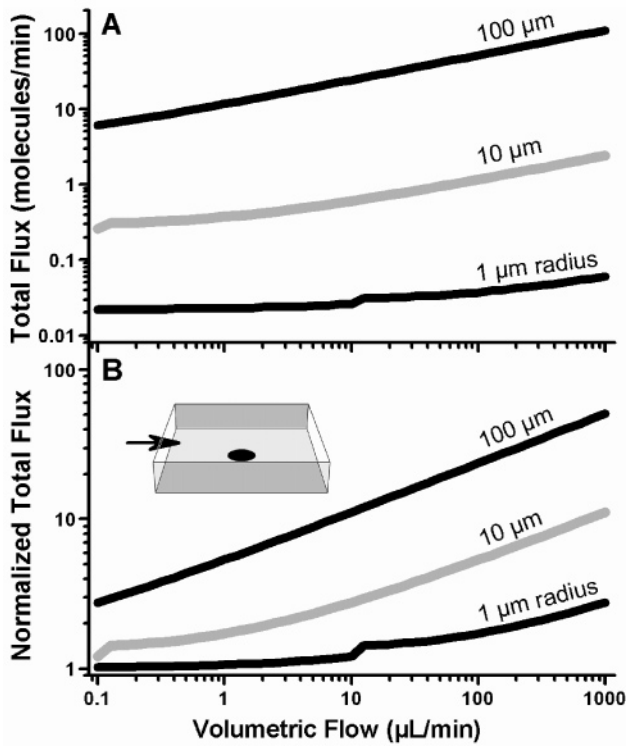

Figure 3. (A) Total flux to a disk sensor in a microchannel at different volumetric flow rates. The radius of the disk is stated; the microchannel is 800 μm wide and 100 μm high. (B) The same data normalized against the steady-state value without flow per eq 4. Flow is not effective at increasing total flux to smaller sensors. The inset illustrates the sensor geometry.

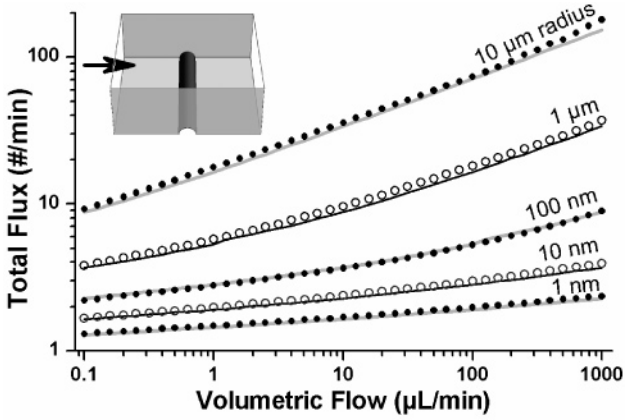

Figure 4. Total flux of molecules to a hemicylindrical sensor in a microchannel. The total flux plotted is the steady-state value at the given volumetric flow rate for a 1 fM concentration. The points (●, ○) are the results of a FEA calculation for a hemicylinder. The lines are calculated using the analytic expression (eq 7) for a rectangular sensor with the same length and surface area as the corresponding hemicylinder (i.e., $W = \pi a$). The sensor is 800 μm long and with the stated radius; the microchannel is 800 μm wide and 100 μm high. The inset illustrates the sensor geometry.

increased only by a factor of ~3. This difficulty stems from the mechanism through which flow increases total flux. For laminar flow in a microchannel, the fluid moves most rapidly in the middle of the channel. The more rapid flow effectively injects undepleted solution into the middle of the channel, thereby compressing the concentration gradient and replen-

ishing any analyte adsorbed as the fluid moves across the sensor. Small sensors, however, already have high concentration gradients and do not significantly deplete the solution, so the enhancement due to fluid flow becomes insignificant for disk sensors less than ~10 μm across. The decreased effect of flow with radius is also present for wire-like sensors (Figure 4), with the effect for a wire with a 10 μm radius being comparable to that for a disk with a 10 μm radius.

As in the static case, some scientists have enhanced mass transport by rethinking the use of convection. Simply decreasing the channel height, h, would increase the effectiveness of fluid flow if the same volumetric flow rate could be maintained. However, the pressure required to maintain the volumetric flow rate[28] increases as $1/h^3$ such that, under practical pressures, the volumetric flow is reduced and the total flux to the sensor diminished. A second approach to obtaining the benefits of high volumetric flow but with a limited analyte volume is to compress the analyte flow with a higher velocity stream directly above the analyte stream in the same channel.[29] A final fluidic approach to increasing the sensor flux is to flow the analyte through the sensor surface by using a nanoporous membrane,[30] thereby directing the analyte directly to the sensor rather than merely streaming it past.

Developers of biosensor devices have reported many elegant approaches to detection, often emphasizing the minimum number of target species or labels that can be detected, with "single molecule" detection the implicit goal.[8−11,31] Because the sensor signal-to-noise ratio increases with decreasing size for many devices (e.g., for microfabricated cantilevers), some researchers are expending considerable effort to fabricate smaller devices.[32−34] Although unique applications certainly exist for nanoscale sensors, if the goal is overall sensitivity, this approach may be misguided. Our results suggest that the appropriate approach is to examine the increase in S:N relative to the critical dimension of the sensor.[35] Taking the case of a disk sensor (eq 4), if the S:N increases slower than the decrease in the sensor radius, one will have to wait longer for the requisite number of molecules for positive detection. Thus, overall sensitivity is diminished and miniaturization is an inappropriate strategy. Even if the S:N scales with the critical dimension, larger sensors are preferred because flux to the sensor may be easily increased via fluidic flow. For most practical applications, we believe the focus should be on the minimal concentration detectable per unit time.

We conclude that detection schemes based solely on static or conventional microfluidic delivery of analyte to micro- or nanoscale sensing zones are unlikely to exceed the ~fM range for assays performed in minutes.[3,4] In all cases, researchers must consider the limits imposed by analyte transport in fluidic systems when designing biomolecular sensors for ultrahigh sensitivity applications.

Acknowledgment. This work was supported by TSWG and DTRA.

Supporting Information Available: Analytic solutions to flow past a sensor and FEA simulations including flow parameters and boundary conditions. This material is available free of charge via the Internet at http://pubs.acs.org.

References

(1) Reyes, D. R.; Iossifidis, D.; Auroux, P. A.; Manz, A. *Anal. Chem.* **2002**, *74*, 2623−2636.
(2) Auroux, P. A.; Iossifidis, D.; Reyes, D. R.; Manz, A. *Anal. Chem.* **2002**, *74*, 2637−2652.
(3) Tamanaha, C.; Colton, R.; Miller, M.; Piani, M.; Rife, J.; Sheehan, P.; Whitman, L. In *Micro Total Analysis Systems 2001*; Ramsey, J. M., van den Berg, A., Eds.; Kluwer Academic Publishers: Boston, 2001; pp 444−446.
(4) Cao, Y. W. C.; Jin, R. C.; Mirkin, C. A. *Science* **2002**, *297*, 1536−1540.
(5) Ferguson, J. A.; Steemers, F. J.; Walt, D. R. *Anal. Chem.* **2000**, *72*, 5618−5624.
(6) Cui, Y.; Wei, Q. Q.; Park, H. K.; Lieber, C. M. *Science* **2001**, *293*, 1289−1292.
(7) Kong, J.; Franklin, N. R.; Zhou, C.; Chapline, M. G.; Peng, S.; Cho, K.; Dai, H. *Science* **2000**, *287*, 622−625.
(8) Ilic, B.; Craighead, H. G.; Krylov, S.; Senaratne, W.; Ober, C.; Neuzil, P. *J. Appl. Phys.* **2004**, *95*, 3694−3703.
(9) Graham, D. L.; Ferreira, H.; Bernardo, J.; Freitas, P. P.; Cabral, J. M. S. *J. Appl. Phys.* **2002**, *91*, 7786−7788.
(10) Wang, H.; Branton, D. *Nature Biotechnol.* **2001**, *19*, 622−623.
(11) Singh-Zocchi, M.; Dixit, S.; Ivanov, V.; Zocchi, G. *PNAS* **2003**, *100*, 7605−7610.
(12) Booth, J.; Compton, R. G.; Cooper, J. A.; Dryfe, R. A. W.; Fisher, A. C.; Davies, C. L.; Walters, M. K. *J. Phys. Chem.* **1995**, *99*, 10942−10947.
(13) Zhang, W.; Stone, H. A.; Sherwood, J. D. *J. Phys. Chem.* **1996**, *100*, 9462−9464. Note that the stated characteristic flow rate, *U*, is incorrectly equated to Q/6hw. The correct value is 6 Q/hw.
(14) Gupta, A.; Akin, D.; Bashir, R. *Appl. Phys. Lett.* **2004**, *84*, 1976−1978.
(15) We focus on biomolecule detection in solution because it is much more challenging than gaseous chemical detection. First, diffusion of molecules in solution is several orders of magnitude slower than through a gas, and consequently mass transport is slower. Second, the desired detection limits for biological species (<0.1 pM) are typically much lower than for gases (1 ppb~50 pM).
(16) Holt, D.; Rabbany, S. Y.; Kusterbeck, A. W.; Ligler, F. S. *Rev. Anal. Chem.* **1999**, *18*, 107−132.
(17) Phillips, C.; Jakusch, M.; Steiner, H.; Mizaikoff, B.; Fedorov, A. G. *Anal. Chem.* **2003**, *75*, 1106−1115.
(18) Myszka, D. G.; He, X.; Dembo, M.; Morton, T. A.; Goldstein, B. *Biophys. J.* **1998**, *75*, 583−594.
(19) Kankare, J.; Vinokurov, I. A. *Langmuir* **1999**, *15*, 5591−5599.
(20) Strictly speaking, the accumulation used here is the average expected accumulation. For a given experiment, the accumulation of a few molecules will be described by Poisson statistics and will display the large relative variances associated with those statistics.
(21) Stellwagen, E.; Stellwagen, N. C. *Electrophoresis* **2002**, *23*, 2794−2803.
(22) Edelstein, R. L.; Tamanaha, C. R.; Sheehan, P. E.; Miller, M. M.; Baselt, D. R.; Whitman, L. J.; Colton, R. J. *Biosens. Bioelectron.* **2000**, *14*, 805−813.
(23) Schena, M.; Shalon, D.; Heller, R.; Chai, A.; Brown, P. O.; Davis, R. W. *PNAS* **1996**, *93*, 10614−10619.
(24) Crank, J. *The Mathematics of Diffusion*; Oxford University Press: Oxford, 1975.
(25) Interestingly, this enhancement may have been overlooked in the explanation of the rings seen when DNA arrays are exposed to a static sample solution. The rings are often attributed to the "coffee stain effect" occurring during spotting, which would result in an uneven distribution of probe DNA.; however, in a static solution, a ring is the expected result.
(26) Carslaw, H. S.; Jaeger, J. C. *Conduction of Heat In Solids*; Clarendon Press: Oxford, 1959.
(27) Heller, M. J.; Forster, A. H.; Tu, E. *Electrophoresis* **2000**, *21*, 157−164.
(28) Brody, J. P.; Yager, P.; Goldstein, R. E.; Austin, R. H. *Biophys. J.* **1996**, *71*, 3430−3441.
(29) Hofmann, O.; Voirin, G.; Niedermann, P.; Manz, A. *Anal. Chem.* **2002**, *74*, 5243−5250.
(30) Lee, G. U.; Yanavich, C. U.S. Patent 6, 676, 904, 2004.

(31) Ilic, B.; Yang, Y.; Craighead, H. G. *Appl. Phys. Lett.* **2004**, *85*, 2604−2606.
(32) Viani, M. B.; Schaffer, T. E.; Chand, A.; Rief, M.; Gaub, H. E.; Hansma, P. K. *J. Appl. Phys.* **1999**, *86*, 2258−2262.
(33) Fritz, J.; Baller, M. K.; Lang, H. P.; Rothuizen, H.; Vettiger, P.; Meyer, E.; J. Güntherodt, H.; Gerber, C.; Gimzewski, J. K. *Science* **2000**, *288*, 316−318.
(34) Li, J.; Stein, D.; McMullan, C.; Branton, D.; Aziz, M. J.; Golovchenko, J. A. *Nature* **2001**, *412*, 166−169.
(35) Rife, J. C.; Miller, M. M.; Sheehan, P. E.; Tamanaha, C. R.; Tondra, M.; Whitman, L. J. *Sens. Actuators, A* **2003**, *107*, 209−218.

NL050298X